STEM CELLS®

TISSUE-SPECIFIC STEM CELLS

Biology of Stem Cells in Human Umbilical Cord Stroma: In Situ and In Vitro Surveys

SERCIN KARAHUSEYINOGLU,[a] OZGUR CINAR,[b] EMINE KILIC,[c] FADIL KARA,[d] GUVEM GUMUS AKAY,[e] DUYGU ÖZEL DEMIRALP,[f] AJLAN TUKUN,[g] DUYGU UCKAN,[h] ALP CAN[a,i]

Departments of [a]Histology and Embryology, [e]Medical Biology, and [g]Medical Genetics, Ankara University School of Medicine, Ankara, Turkey; [b]Department of Infertility, Etlik Maternity and Women's Health Research Training Hospital, Ankara, Turkey; [c]Hemosoft Information and Training Services, Middle East Technical University Technopolis, Ankara, Turkey; [d]Department of Obstetrics, Zubeyde Hanim Maternity Hospital, Ankara, Turkey; [f]Ankara University Biotechnology Institute, Central Laboratory, Besevler, Ankara, Turkey; [h]Department of Pediatric Hematology, Bone Marrow Transplantation Unit, Hacettepe University Faculty of Medicine, Ankara, Turkey

Key Words. Human • Umbilical cord • Mesenchymal stem cells • Differentiation • Cytoskeleton

ABSTRACT

Cells in the umbilical cord stroma have gained attention in recent years; however, differentiation to certain lineages in humans has been demonstrated in few studies. Unlike bone marrow MSCs, human umbilical cord stroma cells (HUCSCs) are far from being well characterized. This study attempts to describe proliferation, structural, and differentiation properties of these cells to account for their exceptional nature in many aspects. Cellular dynamics, cellular structure, and the degree of transformations during expansion and differentiation into mesenchymal and neuronal lineages were examined in vitro over a 10-month period. Comparisons with human bone marrow MSCs regarding differentiation were performed. HUCSCs in culture revealed two distinct cell populations, type 1 and type 2 cells, that possessed differential vimentin and cytokeratin filaments. Corresponding cells were encountered in cord sections displaying region-specific localization. α-Smooth muscle actin and desmin filaments, which were evident in cord sections, diminished through passages. No difference was noted regarding type 1 and type 2 cells in differentiation to chondrogenic, adipogenic, and osteogenic lineages, whereas a preferential differentiation was noted in neuronal lineage. Relative success was achieved by production of chondrocytic spheres and osteogenic monolayers, whereas adipocytes were immature compared with bone marrow MSCs. The presence of neuronal markers suggests that they transform into a certain state of maturity under neurogenic induction. Conclusively, HUCSCs retain their original phenotype in culture without spontaneous differentiation, have a limited lifespan, and bear multipotent stem cell characteristics. Given these characteristics, they may be generally considered progenitor cells if manipulated under appropriate conditions and deserve further study to be potentially used in cell-based therapies. STEM CELLS *2007;25:319–331*

INTRODUCTION

Studies carried out over the past two decades have made possible a more exact definition of stem cells, in which they are capable of self-renewal, can differentiate into multiple lineages, and will function in vivo [1]. Much of the knowledge concerning adult stem cells comes from the numerous studies of hematopoietic stem cells of bone marrow. Friedenstein et al. [2] first demonstrated that the cells from the nonhematopoietic compartment of bone marrow could also differentiate into a broad spectrum of lineages. In later studies, the presence of MSCs, also called mesenchymal progenitor cells, is demonstrated not only in bone marrow but also in the stroma of some tissues and organs, such as peripheral blood [3], cord blood [4], trabecular bone [5], adipose tissue [6], and synovium [7]. Nevertheless, the diversity of MSCs and the lack of definitive markers do not simply allow the characterization and identification of these cells in comparison with the hematopoietic ones.

A less examined source for MSCs is the stroma of umbilical cord, also called Wharton's jelly. Originating from extraembryonic mesoderm at day 13 of embryonic development [8], umbilical cord is composed of two arteries and one vein, all of which are surrounded by a unique connective tissue stroma rich in proteoglycans and mucopolysaccharides [9]. Takechi et al. [10] demonstrated that these stromal cells embedded in the collagen-rich matrix are myofibroblasts rather than typical fibroblasts. Furthermore, these myofibroblasts were reported to exhibit differential localization within the cord stroma associated with differential expression of cytoskeletal filaments [11]. The immature cells retaining the ability to proliferate were reported to locate close to the amniotic surface, whereas highly differentiated fibroblasts, namely perivascular cells (PVCs), were found in closer proximity to the umbilical vessels [12].

In recent studies, cord stromal cells were reported to encompass mesenchymal stem cell character [13–16]. Wang et al. [13] induced the differentiation of umbilical cord stromal cells into mesenchymal cell lineages, such as cardiomyogenic, chondrogenic, osteogenic, and adipogenic types. Sarugaser et al. [14]

Correspondence: Alp Can, M.D., Ph.D., Department of Histology and Embryology, Ankara University School of Medicine, Sihhiye, 06100 Ankara, Turkey. Telephone: 90-312-3103010, ext. 369; Fax: 90-312-3106370; e-mail: alpcan@medicine.ankara.edu.tr Received May 15, 2006; accepted for publication October 6, 2006; first published online in STEM CELLS *EXPRESS* October 19, 2006. 1066-5099/2007/$30.00/0 doi: 10.1634/stemcells.2006-0286

showed the isolation, culturing, and differentiation behavior of human perivascular umbilical cells and obtained osteogenic nodules. Fu et al. [15] and Weiss et al. [16] demonstrated the differentiation capacity of human umbilical cord mesenchymal stem cells into dopaminergic neurons. Most recently, Carlin et al. [17] demonstrated some of embryonic stem cell markers, such as Oct-4, Sox-2, and Nanog, for the first time in porcine umbilical cord matrix cells.

For Wharton's jelly cells to be considered an alternative and potential source of stem cells for clinical use, a greater effort must be made in the study of these cells to determine whether they can serve as a prospective reserve of stem cells for use in cell-based therapies. No demonstration of the ability of human umbilical cord stromal cells (HUCSCs) to differentiate into various lineages has been documented so far with respect to characterization of proliferation, structural, and behavioral characteristics during in vitro expansion, nor has there been a comparison with the well-documented characteristics of human bone marrow stromal cells.

This study was designed so as to first characterize cells throughout the period of expansion, a relatively long period covering 50–60 rounds of cell division cycles. The data obtained from the above experiments helped in the determination of in situ correlations of cultured cells and furthermore facilitated the determination of the most optimum point to induce differentiation of HUCSCs into different lineages. This study accomplished the following objectives: (a) documentation of the phenotypic and structural identification of HUCSCs in culture conditions with in situ correlations; (b) characterization of the proliferation of HUCSCs, which make up a heterogeneous cell population having various degrees of stem cell potency; (c) documentation of HUCSC differentiation into a series of mesodermal lineages, such as adipogenic, osteogenic, and chondrogenic cells, as well as into a neuronal precursor; (d) comparison of HUCSCs with bone marrow MSCs, which appear to have lower potency in forming chondrogenic cells but seem to be more successful in forming adipogenic cells.

MATERIALS AND METHODS

Isolation and Expansion of HUCSCs

Ethical approval was obtained from Institutional Ethical Review Board (approval number 69-1780, 2005). Umbilical cords were obtained from consenting patients delivering full-term infants by Caesarian section ($n = 14$) (mean age, 28.3), who faced no complications throughout pregnancy. Fifteen-centimeter-long cords were immersed in sterile Hanks' balanced salt solution supplemented with penicillin (200 units/ml), streptomycin (200 μg/ml), and amphotericin-B (5 μg/ml) and immediately transferred to the laboratory. All chemicals and reagents used in this study were purchased from Sigma-Aldrich (St. Louis, http://www.sigmaaldrich.com) unless stated otherwise. A small block of transversely sectioned cord tissue was fixed in 4% (wt/vol) paraformaldehyde for 24 hours, immersed in 1.2 M sucrose solution as a cryoprotectant, and finally frozen at −60°C for cryosectioning (10-μm thick). The remaining cord was handled under sterile conditions from this point forward. Arteries and vein were removed by blunt dissection, and the remaining tissue was chopped with scissors and scalpels. Tissue pieces were placed in a Dulbecco's modified Eagle's medium (DMEM)-Ham's F-12 (1:1 vol/vol) culture medium supplemented with 10% (vol/vol) fetal bovine serum (FBS) (Biochrom AG, Berlin, http://www.biochrom.de), collagenase type B (1 μg/ml) (La Roche Ltd., Basel, Switzerland, http://www.roche.com), penicillin (100 units/ml), streptomycin (100 μg/ml), and amphotericin-B (2.5 μg/ml) and digested at 37°C in a gentle orbital shaker until a tissue homogenate was obtained in approximately 4 hours. The homogenate was centrifuged at 500*g* for 20 minutes. The cell pellet was resuspended in the culture medium, and viable cells were counted using a trypan blue dye exclusion assay performed with the Vi-Cell cell analyzer system (Beckman Coulter, Fullerton, CA, http://www.beckmancoulter.com). The total number of viable cells obtained from a 15-cm-long cord was calculated as 4×10^5, and these were seeded to a single 75-cm^2 tissue culture flask (Greiner Bio-One, Frickenhausen, Germany, http://www.gbo.com/en) at a density of 5.3×10^3 cells per square centimeter.

Plated cells were monitored during the first expansion period (passage 0, P_0) for several days before the first passage (P_1). Cell plating density was set at 6×10^3 cells per square centimeter in the first passage (P_1). Cell growth was analyzed by direct cell counts to determine the lag, log, and plateau phases and population doubling time (PDT). Upon reaching 100% confluence, cells in every 75-cm^2 flask were detached using 0.05% trypsin/0.02% EDTA in phosphate-buffered saline (PBS) (Biochrom AG). Flow cytometric analysis for certain MSC markers, such as CD105, CD44, and CD73, all conjugated with either fluorescein isothiocyanate (FITC) or phycoerythrin (PE), was used. Hematopoietic cells were excluded by sorting for CD45, CD34, and CD14 conjugated with PE. FITC-conjugated HLA-DR was also applied (all obtained from Becton, Dickinson and Company, Franklin Lakes, NJ, http://www.bd.com).

To determine the mitotic frequency in cultured HUCSCs, the mitotic cell index was calculated in the middle of *log* phase. The fraction of mitotic cells relative to the total number of cells scored was taken as the mitotic cell index. Cells grown on glass coverslips were fixed and extracted in a fixation/extraction buffer containing 2% (vol/vol) formaldehyde, 0.5% (vol/vol) Triton X-100, 1 mM paclitaxel, 10 U/ml aprotinin, and 50% (vol/vol) deuterium oxide for 20 minutes at 37°C as reported elsewhere [18] and were subsequently stained with the fluorescent DNA dye Hoechst 33258 (details described below). Approximately 1,000 cells were counted on each coverslip. Prophase through telophase figures were counted in captured fluorescent images under a Carl Zeiss Axioimager M microscope (Jena, Germany, http://www.zeiss.com) using Axiovision automated cell imaging software, version 4.3. The remaining coverslips were kept at 4°C in 0.02% (wt/vol) sodium azide containing PBS until they were processed for further imaging.

To test whether cultured cells display tumorigenic transformation throughout a relatively long period of time, their anchorage dependence, loss of contact inhibition, and serum requirement were assessed. Anchorage dependence was tested by culturing two groups of P_7 cells initially plated onto culture dishes. One group of plates was subjected to continuous shaking (20 rpm in an orbital shaker at 37°C in a 5% CO_2 environment), whereas the cells in the other group were left for attachment. Both groups were monitored for 48 hours. Harvested cells were counted to determine the growth rate under these two different conditions.

Loss of contact inhibition and limitation of growth rate were assessed by microscopic observations and time-lapse recording of growth phase. Tested cells were never allowed to remain at confluence for extended periods.

For the assessment of the optimum concentration of serum supplementation on the growth rate of HUCSCs, a gradual decrease (20%, 10%, 5%, and 0%) in serum concentration in the culture media was used ($n = 6$; samples from different individuals used at given passages; P_4 and P_7).

Freezing and Thawing

The effect of freezing and thawing on cell viability was tested using three groups of viable cells at P_4, P_5, and P_7. Cells were detached and resuspended in a medium composed of DMEM/Ham's F-12 medium supplemented with 10% (vol/vol) FBS and 10% (vol/vol) dimethyl sulfoxide (DMSO). The cell suspension was taken into cryotubes (Greiner Bio-One) during the freezing process. The cryotubes were placed in a Mr. Frosty freezing container (Nalgene Labware, Rochester, NY, http://www.nalgenunc.com), stored at −80°C overnight, and then transferred to −196°C liquid nitrogen. Two weeks later, cells were thawed in a 37°C water bath and immediately counted using a Vi-Cell (Becton Dickinson) cell analyzer system. Exactly the same number of cells (5.8×10^5) were reseeded onto 21-cm^2 tissue culture dishes in DMEM/Ham's F-12 medium supplemented with 10%, 15%, or 20% (vol/vol) FBS,

detached, and counted to monitor the growth rate on the 6th and 10th days after thawing.

Isolation of MSCs of Human Bone Marrow Stroma

Human bone marrow stromal cells were obtained from healthy donors who applied to the hospital for bone marrow transplantation procedures. Bone marrow aspirates (1–3 ml) sent for routine analysis before transplantation were used in this study. The bone marrow aspirate samples were diluted in an equal volume of PBS, and mononuclear cells were isolated from the marrow by density centrifugation using Ficoll (density, 1.077 g/l). The cells were then washed twice with PBS and cultured in a medium consisting of DMEM-low glucose (LG), 10% (vol/vol) FBS, L-glutamine (0.584 g/l), penicillin (100 units/ml), streptomycin (100 μg/ml), and amphotericin-B (2.5 μg/ml) at 37°C in a 5% CO_2 environment. Culture medium was replaced twice a week. Upon reaching confluence in 2 weeks, cells were subcultured by detaching with 0.05% trypsin/0.02% EDTA in PBS (Biochrom AG) and plated at 4×10^3 cells per square centimeter for the following passage. Flow cytometric analysis for certain MSC markers, namely CD105, CD44, CD90, and CD106, conjugated by FITC, was used to characterize isolated bone marrow MSCs, and all markers were found to be positive. Hematopoietic cells were excluded by sorting for CD45, CD34, CD14, CD33, and CD3 conjugated with PE.

Immunocytochemistry

For detection of the spatiotemporal distribution and quantification of various proteins in cord cryosections and cultured HUCSCs during expansion and differentiation, single and multi-immunofluorescent labeling techniques were performed using a series of antibodies raised against major cellular markers for different cell types and nuclear proteins. Mouse monoclonal antibodies to vimentin, pancytokeratin (types 1, 4, 5, 6, 8, 10, 13, 18, and 19) (clone C-11+PCK-26+CY-90+KS-1A3+M20+A53-B/A2), desmin (Santa Cruz Biotechnology Inc., Santa Cruz, CA, http://www.scbt.com), α-smooth muscle actin (ASMA), tetramethylrhodamine B isothiocyanate (TRITC)-phalloidin (specific to F-actin; 35 μg/ml in PBS for 60 minutes), and Hoechst 33258 (specific to A-T base pairs in DNA; 1 μg/ml in 1:1 PBS/glycerol mounting medium) were applied. Cy3-conjugated goat anti-mouse IgG (Jackson Immunoresearch Laboratories, West Grove, PA, http://www.jacksonimmuno.com) and FITC-conjugated goat anti-mouse IgG (Jackson Immunoresearch Laboratories) served as secondary antibodies. Unless otherwise indicated, all antibodies were diluted 1:100 in PBS and incubated for 90 minutes at 37°C in a humidified chamber. Other antibodies used to characterize the cells after in vitro differentiation protocols are given below.

All immunofluorescent antibody labelings and dyes were examined using a Carl Zeiss LSM 510 Meta confocal laser scanning microscope equipped with 488-nm argon ion, 543-nm green helium-neon, and 633-nm red helium-neon laser lines. Three-dimensional images were reconstructed by several consecutive optical sections of various thicknesses (0.25–0.38 μm). Hoechst 33258-labeled nuclei were used to count the cell number in cryosections.

Western Blotting

Total cell extract was removed from cultured HUCSCs using a mixture of cell extraction buffer (Biosource, Camorillo, CA, http://www.biosource.com), proteinase inhibitor cocktail, and 1 mM phenylmethylsulfonyl fluoride. The protein concentration was determined by a detergent-compatible protein assay (Bio-Rad, Hercules, CA, http://www.bio-rad.com). Thirty micrograms of protein were loaded into each lane of a 12.5% SDS-polyacrylamide gel electrophoresis gel [19]. The proteins were electroblotted onto nitrocellulose membrane (Bio-Rad) [20], washed with distilled water, and then incubated in 5% (wt/vol) nonfat dry milk in Tris-buffered saline (TBS) (100 mM Tris, 0.9% NaCl, pH: 7.5) containing 0.1% Tween 20 (TBS-T) for 1 hour to reduce nonspecific binding. Membranes were then incubated with anti-pancytokeratin antibody (described above) for 2 hours at room temperature and washed three times with TBS-T over a total period of 20 minutes. Blots were then incubated in horseradish peroxidase-labeled goat anti-mouse IgG (Bio-Rad) in TBS-T for 1 hour at room temperature followed by 12 washes with TBS-T over a total of 1 hour. A chemiluminescence-detecting reagent (Amersham Biosciences, Piscataway, NJ, http://www.amersham.com) was used to illuminate the blot, and 20- × 20-cm films (Amersham Biosciences) were used to show antibody-bound bands. Immunoblot analyses were quantified using a laser densitometer (Kodak, Rochester, NY, http://www.kodak.com).

Karyotyping and Telomerase Activity

Cells from P_1, P_3, P_5, and P_9 were assessed for karyotype analysis from all samples ($n = 14$) as described elsewhere [21]. Telomerase activity was measured by telomeric repeat amplification protocol (TRAP) assay. Samples ($n = 3$) were transferred into 15-ml tubes and centrifuged at 900 rpm, 4°C for 10 minutes. Pellets were homogenized with 1 ml of PBS and transferred to sterile microtubes. Telomerase activity was measured using TRAPeze kit (InterGen, Burlington, MA, http://www.intergen.com) according to the manufacturer's instructions. Then electrophoresis of polymerase chain reaction (PCR) products in 12.5% polyacrylamide gel was performed at 400 V for 90 minutes. SYBR Green (1/10,000) was used for detection. UV images of all samples were digitized using a Kodak Gel Logic 200 Imaging System to quantify the telomerase activity. Signals on ladder bands corresponding to the TRAP product from all samples were measured with Kodak1D software. Relative telomerase activity was calculated as the ratio of total product generated to internal control for each sample within a lane.

Differentiation Procedures

HUCSCs and human bone marrow MSCs were subjected to certain differentiation induction protocols to evaluate their stem cell potency. For this purpose, a variety of protocols were applied to cells between P_3 and P_7. Given their mesenchymal multipotency, they were initially tested using mesenchymal stem cell differentiation induction methods to activate chondrogenesis, adipogenesis, and osteogenesis followed by the neuronal differentiation.

Chondrogenic Differentiation. Confluent HUCSCs and bone marrow MSCs between P_3 and P_7 on 75-cm^2 tissue culture flasks were detached by 0.05% trypsin/0.02% EDTA in PBS (Biochrom AG), and cell suspensions were divided equally into two tubes, both centrifuged at 120*g* for 10 minutes. Following the removal of trypsin/EDTA, culture media were gently added to tubes without disturbing the cell pellets, which were then allowed to settle down at 37°C in 5% CO_2 in a humidified environment. Upon observing the detachment of cell cluster in few days, both tubes were flipped gently with a fingertip to acquire a single floating cell sphere in each tube. In one tube, the medium was carefully replaced with culture medium (control group), whereas the in other, it was replaced with chondrogenic medium composed of 10 ng/ml TGFβ_3, 100 nM dexamethasone, 50 μg/ml ascorbic acid, 1 mM sodium pyruvate, 6.25 μg/ml insulin, 6.25 μg/ml transferrin, 6.25 ng/ml selenous acid (ITS-Premix; BD Biosciences, San Diego, http://www.bdbiosciences.com), 1.25 mg/ml bovine serum albumin, and 5.35 mg/ml linoleic acid in DMEM-high glucose [22]. Media were changed every 3–4 days, and then cell spheres were fixed on day 21 with 10% buffered-formalin for 24 hours at room temperature. Cryosections (10 μm thick) were stained with toluidine blue and Heidenhain's azan, fast and easy histochemical staining methods to demonstrate extracellular matrix mucopolysaccharides and collagen fibers, respectively [23]. Anti-type I and anti-type II collagen mouse monoclonal antibodies (Lab Vision, Fremont, CA, http://www.labvision.com) diluted 1:50 in PBS were applied for 2 hours, followed by a 2-hour incubation in FITC-conjugated IgG for immunofluorescent imaging.

Adipogenic Differentiation. Subconfluent (90%) cells from P_3 to P_7 of HUCSC cultures and bone marrow MSCs on glass coverslips in six-well plates were treated with 1 μM dexamethasone, 500 μM isobutylmethylxanthine, 60 μM indomethacine, 5 μg/ml insulin in DMEM-LG with 10% FBS. Medium was replaced every 3 days for a 6-week period [24]. On days 21 and 41, cells were fixed in 10% buffered formalin for 10–20 minutes at room temperature and stained with 10% (wt/vol) oil red O for 10 minutes [25]. Hematoxylin was used as nuclear counterstain. Since adipose tissue is a

significant source of plasminogen activator inhibitor-1 (PAI-1) protein, with the bulk of production derived specifically from visceral fat [26], we evaluated mRNA expression of PAI-1 production in our adipogenically induced cells to confirm that they express adipose tissue-specific proteins.

PAI-1 mRNA Quantification with Reverse Transcription-PCR Assay. RNA extraction was performed after detachment of adipogenically induced cells using an RNA isolation kit (Promega, Madison, WI, http://www.promega.com). Briefly, cells were placed in microcentrifuge tubes containing lysis buffer and then centrifuged at 2000*g* for 5 minutes. To eliminate potential genomic DNA contamination, RNA samples were treated with 15 U of DNaseI (Promega) during reverse transcriptase reaction for 15 minutes. Finally, total RNA was resuspended in 25 μl of RNase-free water and was kept at −80°C until analysis. Quantities of RNA were measured by using a NanoDrop ND-1000 spectrophotometer (NanoDrop, Wilmington, DE, http://www.nanodrop.com). All procedures were performed according to the manufacturer's instructions. Total RNA (1 μg) from cell cultures that was subjected to a reverse-transcription reaction using a RNA PCR kit (PerkinElmer Life and Analytical Sciences, Boston, http://www.perkinelmer.com). Quantitative real-time PCR was performed in a Light Cycler (Roche) system using the Plexor qPCR kit as recommended by the manufacturer (Promega). In a total volume of 25 μl, each reaction contained 12.5 μl of reaction mixture consisting Taq DNA-polymerase reaction buffer, deoxyribonucleotide triphosphate mixture, Plexor stain, $MgCl_2$, and Taq DNA polymerase. As a negative control, 5–10 μM each primer and 5 μl of cDNA with nuclease-free water were used. Primer sets were as follows: labeled probe, 5′-FAM-ime-isod C/CCACCGTGCCACTCTCGTTCA-3′; primer, 5′-GGCTGACTTCACGAGTCTTTCAG-3′. Quantification of the targets in the unknown samples was performed using a relative quantification method with external standards. The target concentration is expressed relative to the concentration of a reference of adipose tissue samples.

Osteogenic Differentiation. Confluent bone marrow MSCs between P_3 and P_7 growing on glass coverslips in 24-well plates were subjected to osteogenic medium composed of DMEM-LG with 10% (vol/vol) FBS, 100 nM dexamethasone, 0.2 mM ascorbic acid, and 10 mM β-glycerophosphate [27]. Induced monolayers were fixed with 4% (wt/vol) paraformaldehyde at the end of each week during the following 4 weeks and were labeled with mouse monoclonal anti-osteonectin (Alexis Biochemical, Lausen, Switzerland, http://www.alexis-corp.com), rabbit polyclonal anti-osteopontin (Chemicon, Temecula, CA, http://www.chemicon.com), anti-bone sialoprotein-2 (BSP-2) (Alexis), and anti-osteocalcin (Alexis) antibodies diluted 1:50 in PBS. Cy3-conjugated IgGs were used as a secondary antibody diluted 1:100 in PBS. For the visualization of calcium deposits, fixed cultures were stained with Alizarin red S (pH 4.2) [28] and von Kossa/safranin O [29] after being fixed in 10% formalin for 10–20 minutes at room temperature.

Neuronal Differentiation. Both HUCSCs and bone marrow MSCs on glass coverslips precoated with poly-L-lysine (1 μg/ml) were grown to 50% confluence in DMEM/Ham's F-12 medium supplemented with 10% (vol/vol) FBS. Neuronal differentiation was tested using a slightly modified protocol published by Woodbury et al. [30] as follows. In the preinduction period, cells were cultured for 24 hours in DMEM-LG supplemented with 20% (vol/vol) FBS, followed by the addition of 10 ng/ml basic fibroblast growth factor (bFGF) in the next 24 hours. Induction was started on the 3rd day and lasted 24 hours in a medium composed of 2% (vol/vol) DMSO, 200 μM butylated hydroxyanisole (BHA), 25 mM KCl, 10 μM forskolin, 5 μg/ml insulin, 20 mM valproic acid, and 1 μM hydrocortisone in DMEM-LG. Finally, cells were incubated for an additional 24 hours in neurobasal medium (Gibco, Grand Island, NY, http://www.invitrogen.com) supplemented with 10% FBS, 10 ng/ml epidermal growth factor (EGF), 10 ng/ml bFGF, 1× N_2 supplement (Gibco), 1× B-27 supplement (Gibco), and 2 mM L-glutamine for the maintenance of differentiation. After days 3 and 4, cells were either fixed in a fixation/extraction buffer (described above) for microtubules and intermediate filaments or fixed in 4% (wt/vol) paraformaldehyde for 20 minutes at room temperature for the remaining neuronal markers. Differentiated cells were initially stained with anti-tubulin antibody cocktail (1:1 anti-α- + anti-β-tubulin). To assess neurological differentiation, cells were stained with antibodies against neurofilament-160 (NF-M), nestin (Chemicon), neuron-specific enolase (NSE) (Neomarkers), β-III tubulin (Chemicon), microtubule-associated protein-2 (MAP_2) (Chemicon), neuron-specific nuclear protein (Neu-N) (Chemicon), and glial fibrillary acidic protein (GFAP). All antibodies otherwise stated were diluted 1:100 in PBS and incubated for 90 minutes at 37°C in a humidified chamber. Cy3 goat anti-mouse IgG and FITC goat anti-mouse IgG (Jackson Immunoresearch Laboratories) served as secondary antibodies, were diluted 1:100 in PBS, and were incubated for 2 hours at 37°C in a humidified chamber.

RESULTS

Growth Characteristics of HUCSCs During Expansion Period

Freshly isolated cells (P_0) principally displayed a fibroblast-like appearance over the first 3–4 days of culture (supplemental online Fig. 1A). During the 2nd week, they typically appeared as slender cells with a narrow cytoplasm and few lamellopodia (supplemental online Fig. 1B). After 12–14 days, they grew to 100% confluence (supplemental online Fig. 1C). Accumulated data obtained from 14 P_0 cultures showed that the *lag* phase of those cultures lasts around 6–7 days, leading to 6–8 days of *log* phase (Fig. 1A), where PDT reaches 85 ± 7.2 hours (Fig. 1B). A total of $3.6 \times 10^6 \pm 6 \times 10^5$ viable cells per sample were obtained after P_0, and the total number of cells expanded to $11.5 \times 10^8 \pm 2.3 \times 10^6$ after the subsequent passages in 7 months (Fig. 1C). PDT in these passages declined from 85 ± 7.2 hours at P_0 to 11 ± 1.2 hours at P_7 (Fig. 1B), in agreement with the decrease in duration of mitosis (M-phase of cell cycle) from 51 ± 6.8 minutes (Fig. 1D) to 8 ± 2.4 minutes because of a mitotic index of 1% ± 0.2%. Using flow cytometry, all analyzed HUCSCs were labeled positively for CD105, CD73, and CD44 but negatively for CD45, CD34, CD14, and HLA-DR (supplemental online Fig. 2).

The noticeable reduction in PDT led us to test whether cells have a tendency to transform into a tumorigenic character or not. Anchorage dependence, loss of contact inhibition, and deprivation of serum supplementation in culture media were tested. Anchorage dependence was an absolute requirement for proliferation, demonstrated by a 43% decrease in viable cell number in nonanchored cells compared with a 27% increase in anchored ones.

Contact inhibition was tested by microscopic observations recorded in time-lapse movies. Even though a slight tendency to grow beyond confluence was detected in some samples, especially in cells from P_4 to P_9, contact inhibition of growth was consistently observed almost in all passages from all samples.

Since transformed cells show a serum dependence lower than that of their normal counterparts [31], cell growth was tested in media in which the serum concentration was decreased from 20% to 0%. Serum deprivation, particularly in serum-free samples (88% ± 3.2% decrease) and in 5% FBS samples (12% ± 5.6% increase), did inhibit the cell growth (Fig. 1E), whereas viable cell number increased by 3.4-fold ± 0.3-fold in 10% FBS and 6.4-fold ± 0.5-fold in 20% FBS, which indicated that HUCSCs are strictly serum-dependent. No significant difference was noted between P_3 and P_7 samples in terms of serum dependence.

Freezing and Thawing

A decrease (52% ± 2.3%) in the number of surviving cells in tested passages was noted upon revitalization of frozen cells. The total number of viable cells was calculated to be 5.8×10^5

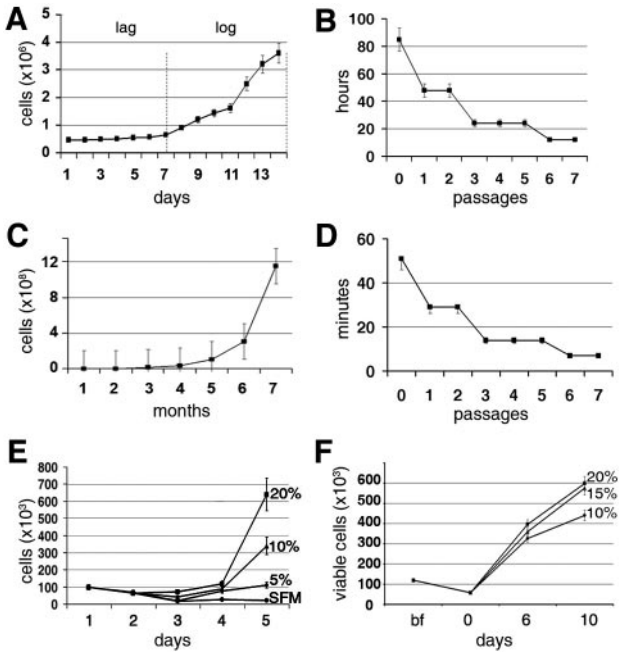

Figure 1. Proliferation characteristics of human umbilical cord stromal cells (HUCSCs) through passage 0 (P_0) to P_7. **(A):** The increase in cell concentration (*y*-axis) through culture days (*x*-axis) in P_0 cells showed that *lag* phase took almost 7 days, followed by a 7-day *log* phase when cells grew exponentially. **(B):** Duration of cumulative population doubling time (PDT) in hours (*y*-axis) is shown through passages (*x*-axis). Note the gradual decrease from 85 to 11 hours. **(C):** Total cell yield during expansion shown per sample reached 11.5×10^8 in 7 months. **(D):** Duration of mitosis (M-phase) in minutes is given. In concordance with PDT, a gradual decrease was noted from 50 to 8 minutes through seven passages. **(E):** Serum dependence of HUCSCs in a given passage was tested using 20%, 10%, 5%, and 0% serum in culture media. SFM and 5% fetal bovine serum (FBS) resulted in an 88% decrease and a 12% increase, respectively, in cell counts, whereas 3.4- and 6.4-fold increases were noted with 10% and 20% FBS at a given passage (P_7). **(F):** Cell survival is given before freezing and at the indicated days after thawing. A slight decrease in the number of viable cells was noted just after thawing, followed by a gradual increase in the subsequent 10 days. Concentration difference (10%, 15%, and 20%) of FBS supplementation after thaw did not significantly alter the growth rate during the 1st week of cultures (as described in Results). After day 6, a higher increase was noted in the 15% and 20% FBS groups. Abbreviations: bf, before freezing; SFM, serum-free media.

$\pm 1.2 \times 10^5$ per group. A rapid increase in cell count was noticed in the following 6 days in three different concentrations of FBS (Fig. 1F). The ratios of the number of total cells versus viable cells were 5.62 ± 0.60, 6.20 ± 0.81, and 6.82 ± 0.76 in 10%, 15%, and 20% FBS, respectively. Cell growth was monitored up to 10 days, at which point, 20% and 15% FBS results were almost similar, whereas the growth rate in 10% FBS-treated cells was 19% $\pm$ 8.2% lower than that of 15% and 20% FBS-treated groups.

Karyotype and Telomerase Activity

For the evaluation of numerical and structural chromosomal abnormalities of HUCSCs, samples from four passages (P_1, P_3, P_5, and P_9) were GTG-banded. None of the samples were found to be abnormal, indicating stable karyotypes between P_1 and P_9 (supplemental online Fig. 3A).

We observed elevated telomerase activity in HUCSCs at the beginning, which declined by $P_{2,3}$. High activation of telomerase at P_4 was downregulated and maintained at a level lower than telomerase-positive HeLa cells by P_5 and P_6 (supplemental online Fig. 3B).

Phenotypic and Structural Characteristics of HUCSCs

P_1 cells initially resembled P_0 cells and showed two distinct morphologies in subsequent days. Some cells possessed widened filopodia, appearing as extremely flattened, stress fiber-rich cells (Fig. 2A, 2B), whereas others were more fusiform in shape, having long cytoplasmic extensions, resembling cells in P_0 subconfluent cultures (Fig. 2A, 2B). We designated these morphological types as type 1 and type 2 cells, respectively. Labeling of intracytoplasmic actin-decorated stress fibers by TRITC-phalloidin clearly displayed the diverse morphology of those two cell types (Fig. 2C) and then led us to characterize them for the possible differential expression of intermediate filament proteins. Cells were first stained with antibodies against vimentin and pancytokeratin, which are mesenchymal and ecto-/endodermal markers, respectively. Interestingly enough, all cells expressed vimentin, whereas pancytokeratin was restricted to type 1 cells (Figs. 2D, 2E, 3E, 3F; Table 1). In addition, we found that there was a decline in the number of type 1 cells through subsequent passages, which coincided with the diminishing expression of pancytokeratin as clearly demonstrated by Western blot analysis between P_3 and P_8 (Fig. 2F; Table 1). The occasional observation of multinucleated cells of P_2–P_{11} led us to consider that these cells arise from fusion of type 1 or type 2 cells.

Since the origin of these cells was the umbilical cord stroma, examination of the cells in their natural environment for those intermediate filaments would be interesting to address whether any differential expression of vimentin in comparison with pancytokeratin coexists in situ. Vimentin was expressed in the cells of both perivascular and intervascular stroma (Fig. 3A), whereas pancytokeratin was markedly found in PVCs rather than in the cells of the intervascular region, which we call intervascular cells (IVCs) (Fig. 3B). As described above all cultured HUCSCs expressed well-organized vimentin filaments (Fig. 3E), whereas only type 1 cells exhibited pancytokeratin filaments (Fig. 3F), which may correspond to PVCs of cord stroma.

It was previously reported that desmin and ASMA are among the major intracellular proteins found in a certain population of cells in the cord stroma [11]. Therefore, it would be complementary to address whether there are expressional differences between the cord stroma cells and the cultured HUCSCs in terms of desmin and ASMA filaments. In umbilical cord sections, we found that desmin was expressed in cells from all stromal regions (Fig. 3C). In contrast, ASMA was predominantly found in PVCs and in cells beneath the amniotic membrane, whereas IVCs showed a relatively low amount of ASMA (Fig. 3D). Interestingly, no desmin positivity was noted in HUCSCs during expansion period throughout the entire cultures (P_1–P_{10}) (Fig. 3G). Another interesting phenomenon was that ASMA filaments consistently lacked central cytoplasmic staining in cells of early passages (P_1–P_3) (Fig. 3H), whereas later passages were totally devoid of staining in the entire cytoplasm (Fig. 3I).

All data above are summarized in Table 1. In addition to the cytoskeletal expression of cord cells, three different groups of cells (i.e., PVCs, IVCs, and subamniotic cells) making up the cord stroma were counted to make an assumption regarding the ratio of cells from a given cord sample. In a given cord section, there were $4{,}311 \pm 25$ PVCs, $8{,}953 \pm 58$ IVCs, and $1{,}362 \pm 37$ subamniotic cells. The ratios are given in Table 1.

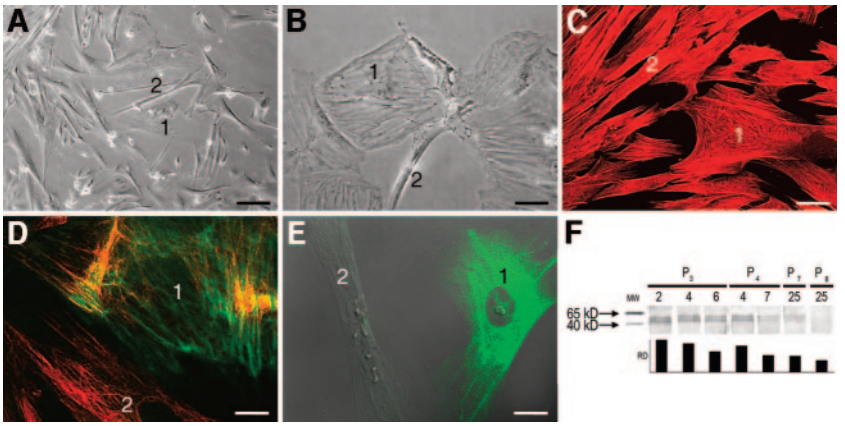

Figure 2. Structural features of different cell types in human umbilical cord stromal cell cultures. **(A, B):** Two distinct cell phenotypes were observed, particularly in early passages (P_1–P_3). Flat, wide cytoplasmic cells (type 1) dispersed among slender, fibroblast-like cells (type 2), marked as 1 and 2, respectively. **(C):** F-actin decoration of type 1 and type 2 cells, which were discriminated by their typical stress-fiber patterns. **(D, E):** Three-dimensional images dual-labeled with anti-pancytokeratin (green) and vimentin (red) showed that pancytokeratin was exclusively expressed in type 1 cells (fluorescent + differential interference contrast images). **(F):** Pancytokeratin gradually diminished through culture days in a particular passage and overall through P_3–P_8. RD of blotted 50–69-kDa proteins is shown. Scale bars = 20 μm **(D)**, 35 μm **(E)**, 50 μm **(B, C)**, 200 μm **(A)**. Abbreviations: kD, kilodalton; MW, molecular weight; P, passage; RD, relative density.

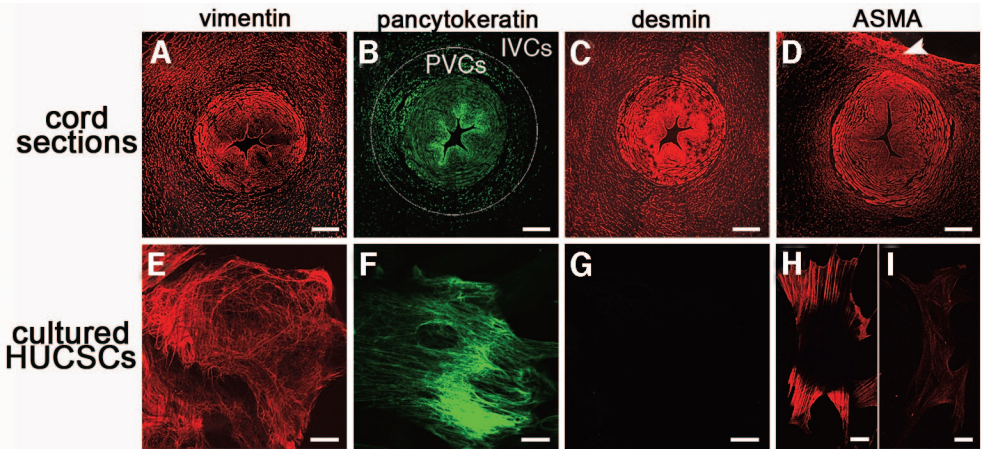

Figure 3. Cytoskeletal co-expressions in stromal cells from umbilical cord sections **(A–D)** and cultured HUCSCs **(E–I)**. **(A):** Vimentin was distributed in the entire cord stroma. **(B):** Pancytokeratin was predominantly found in PVCs, rather than IVCs. **(C):** Desmin expression showed similarity to vimentin, which was expressed by all cell types in the stroma. **(D):** ASMA was preferentially detected in PVCs and subamniotic cells (arrowhead). **(E–I):** Cytoskeletal elements were analyzed in three-dimensional confocal images in cultured HUCSCs. **(E):** Elaborate vimentin filaments were detected in all cells. **(F):** Pancytokeratin was solely found in extremely flat (~3.5 μm thick) type 1 cells. **(G):** Consistently, no desmin was noted in any of the cells cultured. **(H):** ASMA was found in a collar fashion only in early passages (P_1–P_3). **(I):** Later passages were totally devoid of ASMA. Scale bars = 20 μm **(E–H)**, 50 μm **(I)**, and 500 μm **(A–D)**. Abbreviations: ASMA, α-smooth muscle actin; HUCSC, human umbilical cord stromal cell; IVC, intervascular cell; PVC, perivascular cell.

Table 1. Summary of phenotypic and structural characteristics of HUCSCs in situ and in vitro

	Cell number (%)[a]	Vimentin	Pancytokeratin	Desmin	ASMA
In situ HUCSCs					
Perivascular cells	29.4	Strong	Strong	Strong	Strong
Intervascular cells	61.2	Strong	Weak	Strong	Weak
Subamniotic cells	9.4	Strong	Strong	Strong	Strong
In vitro HUCSCs					
Type 1	~50 (≥10)[b]	Strong	Strong	None	Strong
Type 2	~50 (≤90)[b]	Strong	None	None	None

[a]In a given cord section.
[b]First number indicates early passage; number in parentheses indicates late passage.
Abbreviations: ASMA, α -smooth muscle actin; HUCSC, human umbilical cord stroma cell.

Differentiation of HUCSCs to Mesenchymal Lineages

Chondrogenic Differentiation. In the chondrogenically induced groups, cells gathered, forming spherical, shiny-surfaced cell masses of 1–2 mm in diameter within 3 weeks (Fig. 4A). Noninduced samples formed nonshiny, smaller, bulky cell masses (Fig. 4B). Toluidine blue-stained cryosections showed irregular groups of cells embedded in a heterogeneous metachromatic matrix surrounded by a thin capsule (Fig. 4C). Since the metachromatic character of proteins in toluidine blue stain is a fine indicator of mucopolysaccharides, these regions were considered the accumulation of extracellular matrix composed of mucopolysaccharides, the dominant molecule in chondro-

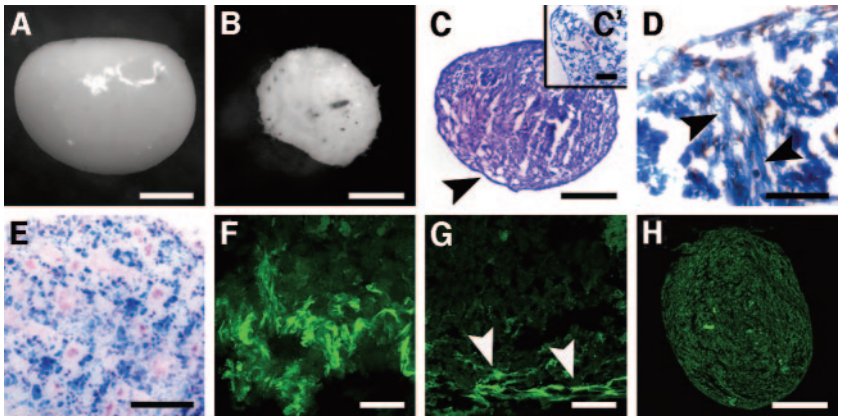

Figure 4. Chondrogenically induced human umbilical cord stromal cells (HUCSCs) formed tiny cell spheres. **(A):** A shiny-surfaced cell mass. **(B):** Noninduced cells formed smaller, bulky cell masses. **(C):** Toluidine blue stain shows the mucopolysaccharide-rich extracellular matrix (pinkish metachromatic areas) and a clear capsule surrounding the entire sphere (arrowhead). **(C′):** No metachromasia was noted in irregular masses of noninduced cells. **(D):** In azan-stained cell masses, collagen fibers were clearly distinguished (arrowheads) among many chondrocytes (nuclei in pale red). **(E):** In cell masses built by the induction of bone marrow MSCs, cells appeared as small groups. Abundant type II **(F)** and few type I collagen fibers **(G)** (arrowheads) were detected in chondrogenically induced HUCSCs. **(H):** Only a few type II collagen fibers were noted in induced bone marrow MSCs. Scale bars = 50 μm **(F, G)**, 100 μm **(D, E)**, 200 μm **(C′)**, and 500 μm **(A–C)**.

genic matrix. Unlike the differentiated cells, the cells in control groups were loosely arranged in highly fragile irregular cell masses without any sign of metachromasia (Fig. 4C′). Azan-stained cell masses in induced groups displayed prominent collagen fibers (Fig. 4D). Similar kinds of cell spheres, albeit more irregular in shape, were obtained from bone marrow MSCs. Figure 4E shows one of the rarely spherical cell masses of bone marrow MSCs, in which cells tend to congregate in small groups and build a poorly filamentous extracellular matrix.

Given that collagen type II is the most abundant collagen form in chondrogenic matrix, differentiated cells were also examined for their collagen production. Type II collagen was found as fine intercellular fibers, the main fibrillar constituent of extracellular matrix (Fig. 4F) only in the chondrogenically induced groups, whereas in nondifferentiated cells, no staining was observed. Interestingly, a few bundles of type I collagen fibers were also detected in chondrogenically induced cell masses, especially in the peripheral zones (Fig. 4G, arrows). In contrast, induced cells of bone marrow MSCs did not show any sign of type I collagen but showed faint staining with type II collagen (Fig. 4H), consistent with the findings in azan-stained sections.

Adipogenic Differentiation. Adipogenic differentiation of HUCSCs was achieved in 40 days, a relatively longer period compared with the bone marrow MSCs. Adipocytic phenotypes in induced HUCSCs were first signaled by the appearance of multisized, tiny intracytoplasmic lipid droplets in fusiform-shaped cells (Fig. 5A). Shortly after, most cells transformed into a more round or cuboid shape (Fig. 5B, 5C) and retracted their cellular extensions, although a few retained their fusiform shape. Lipid granules tended to unite, forming larger ones in the following weeks (Fig. 5D), whereas MSCs produced rounder cells having numerous, homogeneous lipid droplets in 21 days (Fig. 5C, arrows). Although they were cultured for up to 40 days, HUCSCs did not produce a mature adipocyte phenotype compared with relatively more mature bone marrow MSCs. In the nondifferentiated control groups, lipid droplets were not detected at all (Fig. 5F). PAI-1 mRNA levels detected by reverse transcription-PCR showed a 3.8-fold increase in adipogenically induced groups relative to noninduced ones (Fig. 5F).

Osteogenic Differentiation. HUCSCs exposed to osteogenic medium for 3–4 weeks were characterized by their distended

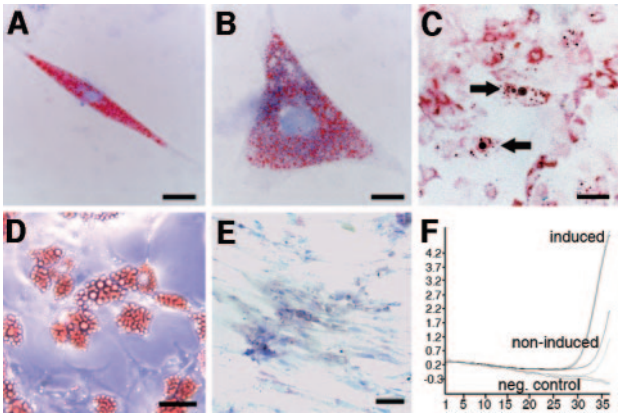

Figure 5. Adipogenic differentiation of human umbilical cord stromal cells. **(A):** Adipocytic phenotypes were signaled by the appearance of multisized, tiny intracytoplasmic lipid droplets stained with oil red O in fusiform-shaped cells. **(B, C):** Shortly, most cells transformed into a more round or cuboid shape. Some lipid droplets united to form larger ones in the following weeks **(C)** (arrows), whereas MSCs produced rounder cells having numerous, larger lipid droplets in 21 days **(D)**. **(E):** In the nondifferentiated control groups, lipid droplets were not detected at all. **(F):** Amplification curves of plasminogen activator inhibitor-1 mRNA in induced, noninduced, and neg. control samples. An increase of 3.8-fold was noted in induced groups relative to noninduced ones. *x*-axis, reverse transcription-polymerase chain reaction cycles; *y*-axis, fluorescence (530 nm). Scale bars = 20 μm **(A, B)** and 100 μm **(C–E)**. Abbreviation: neg., negative.

cell bodies in close proximity to each other. Alizarin red S and von Kossa stains specific for calcium mineralization showed direct evidence of calcium deposits as amorphous accumulations between cells toward the end of 4th week (Fig. 6A, 6B). Safranin O as a counterstain demonstrated the osteoid formation. Noninduced cultures did not exhibit any calcium deposits (Fig. 6A′). Bone marrow MSCs produced abundant calcium deposition after the 4th week of osteogenic induction (Fig. 6A″), implying a generalized mineralization of monolayers.

Attempts were made to identify series of osteocytic proteins in differentiated cells. Osteopontin was the earliest to appear after the 1st week of osteogenic induction as a fine punctate pattern on the cell surface (Fig. 6C). Two weeks later, osteonectin, osteocalcin, and BSP-2 appeared when the osteogenic in-

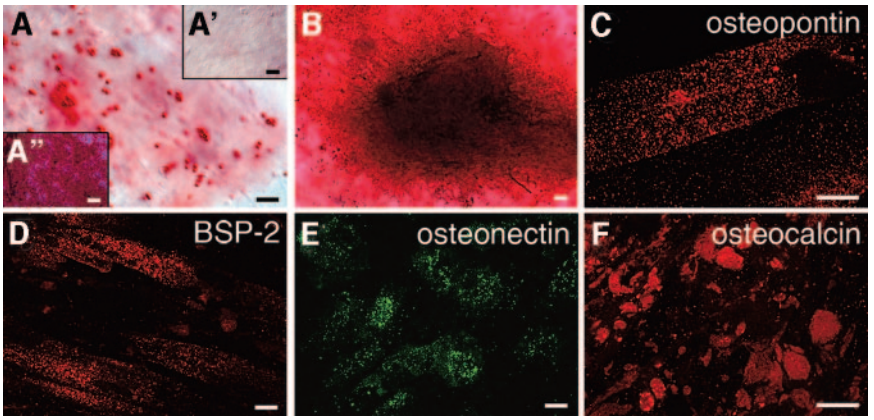

Figure 6. Osteogenic differentiation of human umbilical cord stromal cells. Calcium deposition and osteoid formation as shown by Alizarin red S **(A)** and von Kossa/safranin O stains **(B)** gradually increased up to 4 weeks, whereas no calcium was noted in controls **(A′)**. **(A″):** Disseminated calcium mineralization was noted in induced bone marrow MCS cultures. Osteopontin **(C)**, BSP-2 **(D)**, and osteonectin **(E)** markedly appeared in punctate fashion during the 1st, 3rd, and 4th weeks, respectively. **(F):** Osteocalcin was noted as amorphous patches on calcified monolayers. Scale bars = 20 μm. Abbreviation: BSP-2, bone sialoprotein-2.

duction had almost been completed. BSP-2 (Fig. 6D) and osteonectin (Fig. 6E) were found in a fashion similar to osteopontin, whereas osteocalcin appeared as irregular foci among osteogenic cells (Fig. 6F).

Differentiation of HUCSCs to Neuronal Lineage

Neuronal differentiation of HUCSCs was achieved by a multistep protocol. In the preinduction period, 30%–40% confluent cells exhibited minor phenotypic changes (Fig. 7A). Although fusiform shapes dominated, a small portion of cells in the later hours of preinduction began to show a bulbous appearance with further elongation of several cytoplasmic extensions (Fig. 7B). A composite medium consisting of KCl, valproic acid, insulin, hydrocortisone, BHA, and DMSO, used for neurogenic induction, was applied for 24 hours. The early changes that occurred within 2 hours after replacement of induction medium involved the rounding of cell bodies, giving rise to thin extensions touching each other to a certain extent (Fig. 7C). In the following 5–8 hours, those extensions became thinner and showed bipolarization. One or two longer extensions emanated from the cell body, indicative of the delicate structural organization of axons (Fig. 7D, 7E). Transmission electron microscopic studies revealed that cell nuclei were evidently rich in euchromatin (data not shown), which is a sign of high metabolic activity. Of interest was the observation that, following the 24 hours of differentiation, cells showed signs of dedifferentiation, in which they transformed back to the mesenchymal phenotype, as evidenced by the transformation of round cell bodies into flat ones and the disappearances of axono/dendritic extensions, consequently giving rise to fusiform and fibroblastoid cells (Fig. 7F). Although a maintenance medium including EGF, bFGF, N2, B27 supplements, and L-glutamine was used to overcome this phenomenon, no success was achieved.

During differentiation of cells to the neuronal phenotype, we observed that type 1 cells, described in detail above, responded to induction medium to a lesser extent or not at all (Fig. 7H). The wide and flat cytoplasm of those cells did not transform into a round shape. Most of them showed very short extensions without any formation of axon- or dendrite-like structures. In contrast, type 2 cells, which dominated in later passages, as shown in Figure 7A, did show a differentiation pattern consistent with a neuronal phenotype.

Anti-tubulin antibody, which recognizes dimeric proteins of microtubules, was used as a tool to illuminate the overall morphology of induced and noninduced cells. Microtubules were found along the extensions and elaborations of rounded cell bodies (Fig. 7G). The difference between type 1 and type 2 cells was dramatically observed in the typical appearance of those cells (Fig. 7H), as described above. To confirm the extent to which induced cells possess neuronal features, they were stained with antibodies against proteins specific to neuronal precursors or mature neurons. MAP_2, a dendrite-specific protein prominent in mature neurons, was positive as several patches within perikarya and in cell extensions in induced cells (Fig. 7I, 7J), but it was not detected in the noninduced control group. β-III tubulin, a marker of developing neurons, was observed in both cell bodies and neuronal outgrowths of induced HUCSCs (Fig. 7K). Nestin, a high molecular weight intermediate filament present in neuronal precursors, was found in a filamentous fashion that showed the highest intensity in close proximity to the cell nucleus (Fig. 7L, 7L′). Noninduced cells were completely negative for nestin. Neurofilament-M, a neuronal intermediate filament protein, was also positive, especially in cells having bipolar orientation (Fig. 7M). Neu-N, a specific antigen for neuron cell nucleus, was positive in induced cells (Fig. 7N) and entirely negative in noninduced ones. Only 20%–25% of induced cells revealed NSE positivity as intracytoplasmic patchy pattern (Fig. 7O, arrows), whereas the remaining induced and noninduced cells were faintly stained in a punctuate fashion (Fig. 7O). GFAP, a protein specific for astrocytes, was negative in both induced (Fig. 7P) and noninduced HUCSCs.

Neuronal differentiation experiments using bone marrow-derived MSCs revealed phenotypes similar to HUCSCs. Interestingly, they also transformed into a more fibroblastic nature in 48 hours after induction. During the induction period, cells were characterized by NF-M expression (D. Uckan et al., unpublished data).

DISCUSSION

Although a wide variety of cell markers are used to characterize MSCs, the intrinsic ability of these cells to adhere to uncoated plastic substrates stands as the most consistent property of these cells, regardless of their origin. Besides the well-characterized MSCs, which are derived from bone marrow and cord blood, a growing body of evidence suggests that human umbilical cord matrix contains a substantial amount of cells having properties similar to MSCs. The cord tissue surrounding the blood vessels is typically classified as mesenchymal or embryonic connective tissue [32], so it is reasonable to consider that human cord stromal cells have a stem cell character to some extent. Given the results of the present work and of a few studies [11, 12] reported in the literature in recent years, it is possible to postulate that human umbilical cord stroma cells commit to a certain state in Wharton's jelly during development of cord.

An important issue of interest in adult stem cell studies is the availability of the source and efficacy of isolation techniques to yield a reasonable number of viable cells to expand. Therefore,

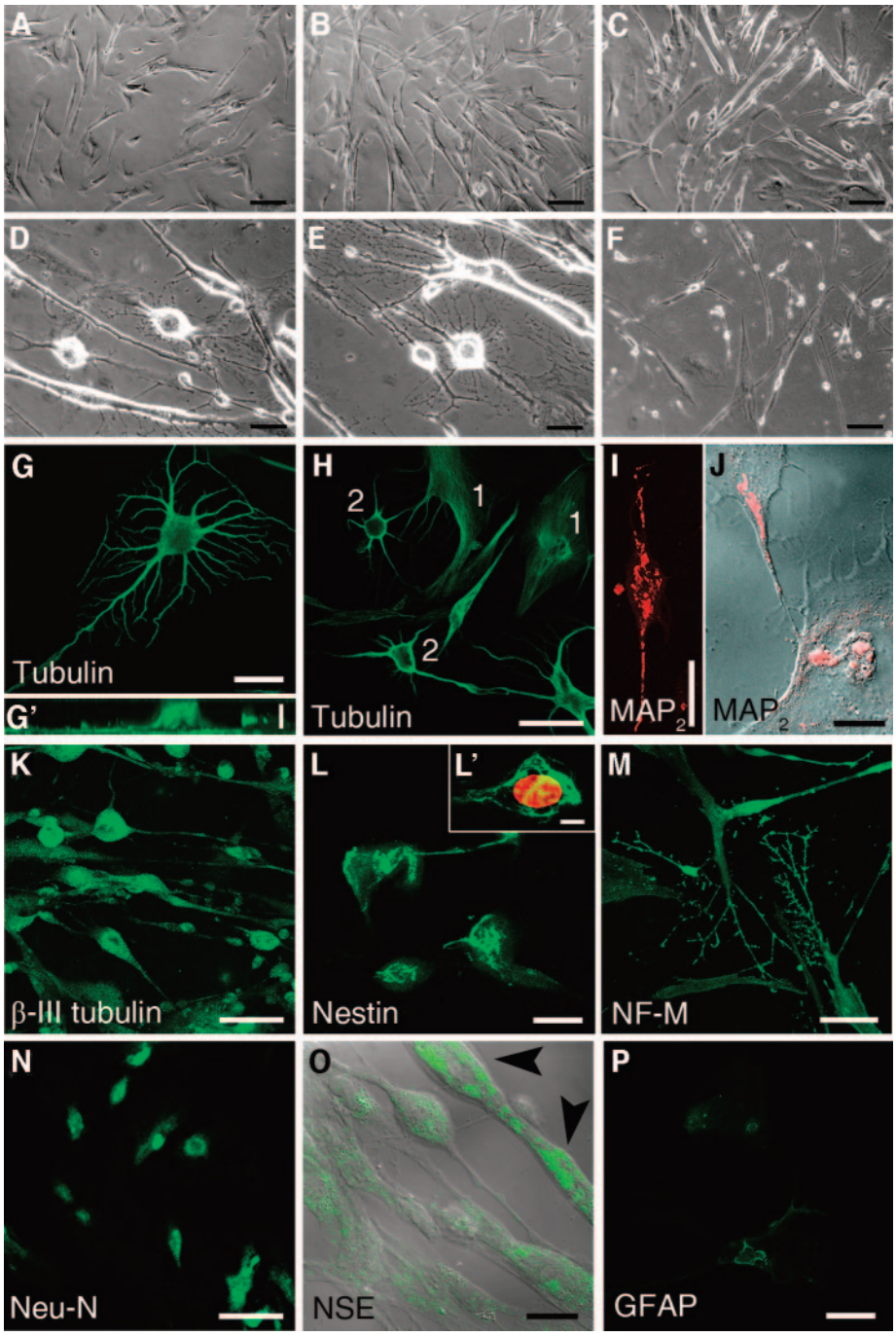

Figure 7. Differentiation of human umbilical cord stromal cells (HUCSCs) to neuronal lineage **(A–F)** and three-dimensional images obtained from consecutive optical sections showing expression of neuronal markers **(G–M)**. Confluence of 30%–40% was found to be most favorable for the onset of preinduction, during which minor changes occurred in early **(A)** and later **(B)** hours. **(C):** By the onset of the induction period, cells suddenly responded, their bodies becoming more slender and extending microspikes. **(D, E):** In the following hours, cells transformed into a neuronal shape having bipolar cell bodies and protrusions resembling axons and dendrites. **(F):** Nevertheless, they did not maintain these phenotypes and transformed into a fibroblastic nature in 48 hours. **(G):** Microtubules were found in cell bodies and along the entire cell extensions. **(G′):** Sections taken in the *x-z* direction in confocal microscope showed that cells had a mean thickness of 16.5 μm. **(H):** Discrepancy between type 1 and type 2 cells in response to neuronal differentiation; no structural alteration was noted in type 1 (1) as opposed to type 2 (2) cells. **(I):** MAP_2 was detected as discontinuities along the cells. **(J):** MAP_2 distribution in cell-cell contact. β-III tubulin **(K)** and NF-M **(M)** were strongly positive throughout the perikarya and extensions. Nestin appeared as a filamentous "nest" **(L)**, located in the perinuclear cytoplasm in particular **(L′)**. **(N):** Neu-N was exclusively restricted to cell nuclei in induced HUCSCs. **(O):** NSE (arrows) appeared as intracytoplasmic patchy areas in some cells, whereas most stained in a weak punctuate fashion. **(P):** GFAP was negative in induced HUCSCs. Scale bars = 10 μm **(L′)**, 15 μm **(G′)**, 20 μm **(J, L, P)**, 50 μm **(D, E, G, I, O)**, 100 μm **(H, K, M, N)**, and 200 μm **(A, B, C, F)**. Abbreviations: GFAP, glial fibrillary acidic protein; MAP_2, microtubule-associated protein-2; Neu-N, neuron-specific nuclear protein; NF-M, neurofilament-160; NSE, neuron-specific enolase.

one of the main focuses of this study was designed to evaluate the efficiency of expansion of those cells with a series of in vitro proliferation parameters before they are induced to differentiate. Although the frequency of bone marrow stromal cells is often reported to range from 1 to 10 MSCs in a total of 10^6 bone marrow mononuclear cells [33–35], the number of MSCs in umbilical cord blood is found to range from 1×10^3 to 5×10^3 cells per sample [4], in addition to the difficulty of isolating and expanding adherent cultures. Because of the results of several isolation and expansion experiments used in this study, it is realistic to claim that the harvesting ratio of MSCs in cord stroma is relatively high (4×10^5 cells per sample; $10–15 \times 10^3$ cells per centimeter of cord). This finding is consistent with the study of Sarugaser et al. [14], in which MSC yield was reported to be 100%, meaning that they harvested cells from every cord received, although they only examined the PVCs of human umbilical cords. Weiss et al. [16] also obtained a 100% yield, with a similar number of cells per centimeter of cord length. Apparently, isolation of any type of tissue-embedded stem cell through a harsh, time-consuming, and costly tissue digestion process stands as a pitfall, as opposed to easy collection and storage conditions of blood-originated stem cells.

One of the striking features of HUCSCs was the capacity to expand cell numbers almost 300-fold over seven passages. However, HUCSCs spent a great deal of time in *lag* and *log* phases (6–7 and 6–8 days, respectively), compared with PVCs obtained from human umbilical cords, which are reported to spend 24 hours in *lag* and 24–120 hours in *log* phase [14]. The

decrease in PDT in subsequent passages was more evident in HUCSCs than in PVCs in the study of Sarugaser et al. [14], in which PDT showed a constant pattern after P_2. We assume that differences in such dynamics may be due to the heterogeneity of HUCSCs, which include all perivascular, intervascular, and subamniotic cell populations. The efficiency of expansion of HUCSCs seems encouraging; nevertheless, the significant decline in PDT and the M-phase period from P_1 to P_7 urged us to examine whether a tumorigenic transformation had occurred. The significant decrease in cell viability in serum-free culture media, the dependence on anchorage, and the cessation of cell growth upon cell-cell contact ruled out the possibility of this phenomenon. A normal karyotype pattern in all passages excluded the major structural chromosomal abnormalities.

Cellular regulation of telomerase is required to keep a balance between normal proliferation capacity and cancer development [36]. HUCSCs showed relatively stable telomerase activity by $P_{1–3}$ and $P_{5,6.}$ Upregulated endogenous telomerase activity at P_4 could be resulted from a clonal expansion, leading to immortalization. In fact, activity was not maintained at high levels because of a lack of major chromosomal abnormalities, which is required for tumorigenic transformation. Taken together, the above data suggest that HUCSCs in culture are safe enough, at least during the tested passages, and do not spontaneously transform into tumorigenic phenotype.

An important finding was that viable cell number decreased slightly after freezing and thawing, even though the remaining viable cells were successfully expanded in consecutive days, indicating that HUCSCs may tolerate freezing and thawing cycles both structurally and metabolically.

Careful examinations of cells in culture interestingly revealed two distinct cell phenotypes, which appeared in early passages in particular. Cellular differentiation in vitro and in vivo is closely connected with morphological changes based on intermediate filament protein remodeling. Intermediate filaments are expressed in cell type-specific patterns following and demarcating pathways of embryonic development and cellular differentiation [37]. Vimentin is a 50-kDa protein found in cells of mesodermal origin, whereas cytokeratins are a group of 55–69-kDa proteins basically found in epithelial cells of ecto-/endodermal origin. The staining frequency and the corresponding phenotype of those cells led us to conclude that isolated and cultured HUCSCs, even though all are mesenchymal stem cells in nature, contain at least two distinct cell populations, which might have been derived from different tissue sites and/or have an embryological origin. In addition to the fact that cytokeratin filaments are solely expressed in cells of ecto-/endodermal origin, during development, some cytokeratin isoforms are expressed in myofibroblastic cells as well. This is particularly true for cytokeratins 8, 17, and 19 [38], which are recognized by the pancytokeratin antibody. Similar findings were also reported for the umbilical cord stroma cells [39]. Therefore, it was not unusual to detect cytokeratin-expressing cells in the present study, which in fact facilitated the characterization of the nature of these cells.

The differential expression of certain cytoskeletal elements in cultured cells led us to examine the umbilical cord sections in situ to see whether a similar disparity in the expression of same cytoskeletal proteins exists in different regions of the tissue. Interestingly, vimentin was distributed evenly in all perivascular and intervascular regions, whereas pancytokeratin showed a clear zonal distribution. Cells surrounding the umbilical cord vessels (i.e., PVCs) showed intense staining, whereas the cells found between the vessels, which we prefer to call "intervascular cells," expressed little or no pancytokeratin. The cuboidal epithelial cells of the amniotic membrane exhibited the strongest staining, as expected. These findings are consistent with those reported by Nanaev et al. [11]. Pancytokeratin-positive cells in culture exhibit the type 1 cell phenotype, but in practice, they do not differentiate into neurons, which are discussed below.

Desmin, a myogenic cytoskeletal protein, revealed a distribution similar to that of vimentin throughout the entire stroma and verified the myofibroblastic character of umbilical cord stroma cells as clearly defined by Takechi et al. [10] and Kadner et al. [40]. In contrast to PVCs described by Sarugaser et al. [14], desmin expression was not detected in isolated cultured cells at any time in the present study until the cells were induced by cardiomyogenic induction medium (supplemental online Fig. 4; manuscript in preparation). The existence of diffuse desmin positivity among all stromal cells in tissue sections, as opposed to the total lack of expression in cultured cells, may reflect the sudden downregulation of desmin synthesis, possibly because of isolation and/or culturing conditions. Convincing evidence arises from the studies of Darby et al. [41], in which wound myofibroblasts have been shown to temporarily not express desmin but only express ASMA. Similar phenomena might also relate to the low expression of ASMA in our continuing subcultures, whereas it was found to be strongly positive in tissue sections and earlier passages, results that are also supported by the findings of Sarugaser et al. [14] and Mitchell et al. [42]. Mitchell et al. [42] also reported that ASMA-positive cells lose ASMA expression when differentiated into neurons.

Cells in human Wharton's jelly are not evenly distributed. The most immature cells, having greater competence to resume proliferation, are located in subamniotic and intervascular regions, whereas cells of perivascular regions mainly constitute the highly differentiated myofibroblasts [11]. Given our results and this site-specific property of stromal cells, we hypothesize that because of their myofibroblastic and highly differentiated features, PVCs leave cultures in an early state where they can no longer contribute to a number of processes related to differentiation, primarily to a neuronal phenotype. On the other hand, less differentiated IVCs and subamniotic cells rapidly lose their weak myofibroblastic character, considering changes in ASMA and desmin expression during in vitro expansion. They therefore transform to a bi-/tri-/multipotent stem cell state, where they gain higher affinity for differentiation. This may account for why late passages, compared with earlier ones, have a higher tendency to respond to induction of neurogenic differentiation.

Based on the notion that a cell is called a "stem cell" because it is capable of giving rise to a more committed cell(s), an attempt to address this question was the second main goal of this study. The formation of chondrogenic micromasses staining positively with common mucopolysaccharide dyes clearly indicated that HUCSCs are able to transform into chondrocytes. De novo synthesis of type II collagen fibers, which are normally synthesized by chondroblasts in various types of chondral tissues in human [43], further indicated the functional differentiation of HUCSCs in cohort behavior without any preference seen in type 1 or type 2 cells. The peripheral localization of a few type I collagen fibers detected in chondrogenic cell masses implies the formation a capsule, which corresponds to perichondrium. Minimal collagen type I production was also reported in chondrogenic differentiation of rabbit MSCs [44]. However, the question still remains of whether external cues or intrinsic factors necessary for chondrogenesis play the major role in determining the amount and/or type of collagen. Weak staining of bone marrow MSCs by type II collagen raises the possibility that chondrogenic potency in these cells is poor compared with that of HUCSCs. Obviously, further evaluation specific to chondrogenic potentials of those two kinds of stem cells is necessary.

When incubated in adipogenic medium, HUCSCs gradually differentiated into multilocular adipogenic cells in vitro, confirmed by an elevated expression of PAI-1, which is a member of serine

proteinase inhibitor family that is highly expressed in adipose tissue, as are adiponectin and resistin [45, 46]. Stained positively with oil red O, these multilocular cells could be considered preadipocytes. Despite receiving exactly the same adipogenic induction medium as with bone marrow MSCs, HUCSCs showed a relatively premature reminiscent appearance, reminiscent of the multilocular forms of adipocytes dominant in brown adipose tissue in the fetus [32]. Similar to many MSCs originating from diverse sources, lipid accumulation in these cells usually did not proceed to the unilocular state, as seen in mature adipocytes. The formation of homogeneous lipid droplet-laden cells produced by bone marrow MSC cultures reveals that these cells have a greater tendency to differentiate into adipocytes in the same culture conditions, as also reported previously [47]. The adipogenic differentiation capacity of human umbilical cord blood stromal cells was also reported to be less than that of bone marrow MSCs [48, 49]. The potency of developing mature adipocytes by bone marrow MSCs versus umbilical cord and cord blood MSCs may be due to the fact that some of the cells in bone marrow stroma are already committed to forming mature adipocytes in situ.

Stem cells of mesenchyme origin are generally accepted as a convenient source for osteoblasts, the cells that synthesize bone matrix. In vitro differentiation of bone marrow MSCs to osteoblasts has classically involved incubating a confluent monolayer of cells with ascorbic acid, β-glycerophosphate, and dexamethasone for 2–3 weeks [2, 50]. Wang et al. [13] demonstrated that cells from the same source used in the present study were able to differentiate into osteopontin-positive cells in vitro in 28 days. More recently, human umbilical cord PVCs were shown to form bone nodules after being cultured in the presence of the above supplements in a 5-day induction period [14]. Here, we report a mixture of PVCs and IVCs in a cohort that successfully underwent osteogenic differentiation in 3 weeks, as indicated by the intense expression of osteopontin, BSP-2, osteonectin, and osteocalcin; the formation of calcium deposits; and osteoid formation. Given the possibility that type 1 cells correspond to PVCs in vivo and the relatively faster differentiation to osteoblasts as shown by Sarugaser et al. [14], these data suggest that different types of cells found in human umbilical cord stroma show variations in differentiating into osteoblasts. Therefore, it is reasonable to raise the possibility that the differences in the duration of osteogenic differentiation reported by Wang et al. [13], Sarugaser et al. [14], and in the present study arise from the diversity of cells used.

Because HUCSCs are mesenchymal in origin, their differentiation into neurons or neuronal precursors is really a matter of interest, since lineage restriction is an important issue in stem cell biology. The rapid change in the morphology of cells in almost 3 hours from a fibroblastic appearance to more round cell bodies characteristic of neurons has also been noted by Woodbury et al. [30]. In the following hours, cells showed bipolarity, followed by multipolarity to some extent. It was interesting to find the expression of MAP_2, a marker of mature neurons, in differentiated HUCSCs. The patchy appearance of inner cytoplasmic MAP_2 localization, as well as its regional distribution in cell-cell contacts, may indicate the onset of the stabilization of microtubules. MAP_2 is known to express at later stages than Neu-N, because of changes during development [51], whereas Neu-N is expressed in a state when terminal differentiation of a neuron occurs [52]. Conflicting results, however, were reported, as MAP_2 was also expressed in undifferentiated bone marrow MSCs [53]. HUCSCs clearly showed no evidence of MAP_2 in the undifferentiated state. The co-expression of both MAP_2 and Neu-N in our study, despite a short duration of incubation, suggests that differentiating neuronal cells reach a state in vitro where they gain a maturity level regardless of the priority of proteins expressed. Apparently, the ultimate MAP_2 orientation would not be completed until the final maturity of neurons is achieved, such as stable growth cone assembly and synapse formation.

Neurofilaments (NF-L, NF-M, and NF-H) are synthesized in the neuronal perikarya, assembled to form filaments, and then slowly transported within the axons toward the synaptic terminals [54]. NF-M was localized both in perikarya and neurites, as reported in previous studies [30, 42], indicating that cells assembled with the basic neuronal structure are consistent with their neuron-like morphology. Nestin, which was initially identified as a marker of neural stem and neural progenitor cells [55], displayed a typical form of nest-like filaments preferentially located around nuclei of differentiated HUCSCs. Contrary to the recent suggestions that nestin may be a common marker of multilineage progenitor cell, in our work, nestin profiles were exclusively confined to neuronally induced cells.

HUCSCs showed a differential expression of NSE; that is, only a few induced cells expressed NSE strongly, whereas most were considered negative, similar to noninduced ones. NSE is the most abundant form of glycolytic enolase found in adult neurons and is thought to serve as a growth factor for neurons [56]. The expectation, therefore, is that NSE might be detected in developing neurons in vitro. Woodbury et al. [30] and Mitchell et al. [42] reported that NSE was expressed in neuronally induced cells. However, they also noted that NSE was also expressed in undifferentiated MSCs of porcine umbilical cord and rat bone marrow stroma cells [30, 42]. The results of these two studies were not identical, since Mitchell et al. [42] reported that NSE expression was almost equal in both undifferentiated and neuronally differentiated cells, whereas Woodbury et al. [30] noted a significant increase of NSE after induction with neurogenic medium. On the other hand, Sarugaser et al. [14] reported that NSE was negative in both induced and noninduced PVCs of human umbilical cord.

β-III Tubulin, one of the six isotypes of β-tubulin polypeptides, is found specifically in brain and dorsal root ganglia and localized to neurons, where its expression seems to increase during axonal outgrowth [57]. Therefore, the expression of β-III tubulin in both cell bodies and neuronal outgrowths of induced HUCSCs is a sign of neuron formation. Since previous studies show that the assembly of $\alpha\beta$-III dimers in presence of MAP_2 is faster [58], expression of MAP_2 with β-III tubulin may coincide with the initiation of a more complex neuronal structure. Lack of β-III tubulin in glia cells, which have β-II and β-IV tubulins instead [59], confirms that the positively stained cells in this study are solely neurons.

Our cells were negative for GFAP, an intermediate filament protein specific for astroglial cells. GFAP was reported positive in both induced [42, 60] and noninduced cells [42] where three different media were used, some of which were different from ours. GFAP was also absent in the bone marrow stromal cells studied by Woodbury et al. [30], who concluded that the medium they used did not support astrocytic differentiation. Since we used a slightly modified version of the medium defined by those authors, it was not surprising that GFAP was negative in induced HUCSCs. Such differences in these results may be associated with the varieties in state of maturity of neurons, as well as the source and character of the cells obtained. As a conclusive remark for all differentiation attempts, we postulate that spatiotemporal differences in many cellular markers reported here and in many studies may be due to the different media and supplement formulations used by different laboratories.

Conclusively, HUCSCs possess a substantial and distinctive capacity to proliferate and differentiate, as demonstrated in detail in the present study. To our knowledge, this is the first study in the literature regarding the following aspects. (a) Growth characteristics of HUCSCs as a heterogeneous cell population are different

from those of the perivascular cells, as reported before. (b) Phenotypically, there are at least two kinds of cells in the cord matrix: type 1 and type 2 cells. (c) Cells in the umbilical cord stroma differ in situ from their in vitro correlates regarding their spatiotemporal cytoskeletal protein distribution. (d) Pancytokeratin expression is solely confined to type 1 cells, which may correspond to perivascular cells that are differentiated myofibroblasts in nature and cannot form neurons in vitro. Therefore, there seems to be a site-specific arrangement for matrix cells in terms of differentiation potency. (e) A significant number of cells are yielded after freeze-thaw cycles. (f) Bone marrow MSCs are more successful in forming adipogenic cells, whereas they have less potency in forming chondrogenic and osteogenic cells compared with HUCSCs. (g) When induced to a chondrogenic lineage, HUCSCs express not only type 2 but also peripherally located type 1 collagen. (h) HUCSCs express immature neuronal and/or immature forms of mature neuronal markers.

Given these many characteristics, particularly the plasticity and developmental flexibility, HUCSCs may well be considered progenitor cells, which are classically defined by a high but limited proliferation capacity and an inability to form tumors [6]. Although culture conditions and supplements seem sufficient, they are far from matching the physiological signals cells received that induce differentiation in vivo. Undoubtedly, further evaluation is needed to understand the functional nature of in vitro differentiated HUCSCs, and particularly their in vivo physiology, before going through long-term phase clinical tests. It is also important to know whether or not these cells that will adopt a new fate will maintain their fate throughout the life of the tissue and not revert to the embryonic origin.

ACKNOWLEDGMENTS

We thank Prof. Asuman Sunguroglu and Pinar Ozkal for help in karyotype analyses, Esra Erdemli for criticism in preparation of the project proposal, and Dr. Mitch Halloran for phrasing suggestions. This study was financially supported by Ankara University Biotechnology Institute Project 2005-180 and TUBITAK SBAG-3314.

DISCLOSURES

The authors indicate no potential conflicts of interest.

REFERENCES

1 Verfaillie C. Adult stem cells: Tissue specific or not? In: Lanza R, ed. Essentials of Stem Cell Biology. Oxford, U.K.: Elsevier Academic Press, 2006;23–27.
2 Friedenstein AJ, Chailakhyan RK, Latsinik NV et al. Stromal cells responsible for transferring the microenvironment of the hemopoietic tissues. Cloning in vitro and retransplantation in vivo. Transplantation 1974;17:331–340.
3 Zvaifler NJ, Marinova-Mutafchieva L, Adams G et al. Mesenchymal precursor cells in the blood of normal individuals. Arthritis Res 2000;2: 477–488.
4 Rogers I, Casper RF. Umbilical cord blood stem cells. Best Pract Res Clin Obstet Gynaecol 2004;18:893–908.
5 Noth U, Osyczka AM, Tuli R et al. Multilineage mesenchymal differentiation potential of human trabecular bone-derived cells. J Orthop Res 2002;20:1060–1069.
6 Pittenger MF, Mackay AM, Beck SC et al. Multilineage potential of adult human mesenchymal stem cells. Science 1999;284: 143–147.
7 De Bari C, Dell'Accio F, Luyten FP. Human periosteum-derived cells maintain phenotypic stability and chondrogenic potential throughout expansion regardless of donor age. Arthritis Rheum 2001; 44:85–95.
8 Sadler TW. Second week of development: Bilaminar germ disc. In: Sadler TW, ed. Langman's Medical Embryology. 9th ed. Philadelphia: Lippincott Williams & Wilkins, 2004;57.
9 Sobolewski K, Bankowski E, Chyczewski L et al. Collagen and glycosaminoglycans of Wharton's jelly. Biol Neonate 1997;71:11–21.
10 Takechi K, Kuwabara Y, Mizuno M. Ultrastructural and immunohistochemical studies of Wharton's jelly umbilical cord cells. Placenta 1993; 14:235–245.
11 Nanaev AK, Kohnen G, Milovanov AP et al. Stromal differentiation and architecture of the human umbilical cord. Placenta 1997;18:53–64.
12 Benirschke K, Kauffman P. Anatomy and pathology of the umbilical cord and major fetal vessels. In: Benirschke K, Kauffman P, eds. The Pathology of The Human Placenta. 4th ed. New York: Springer-Verlag, 2000;335–398.
13 Wang HS, Hung SC, Peng ST et al. Mesenchymal stem cells in the Wharton's jelly of the human umbilical cord. STEM CELLS 2004;22: 1330–1337.
14 Sarugaser R, Lickorish D, Baksh D et al. Human umbilical cord perivascular (HUCPV) cells: A source of mesenchymal progenitors. STEM CELLS 2005;23:220–229.
15 Fu YS, Cheng YC, Lin MY et al. Conversion of human umbilical cord mesenchymal stem cells in Wharton's jelly to dopaminergic neurons in vitro: Potential therapeutic application for Parkinsonism. STEM CELLS 2006;24:115–124.
16 Weiss ML, Medicetty S, Bledsoe AR et al. Human umbilical cord matrix stem cells: Preliminary characterization and effect of transplantation in a rodent model of Parkinson's disease. STEM CELLS 2006;24:781–792.
17 Carlin R, Davis D, Weiss M et al. Expression of early transcription factors Oct4, Sox2 and Nanog by porcine umbilical cord (PUC) matrix cells. Reprod Biol Endocrinol 2006;4:8.
18 Can A, Semiz O, Cinar O. Centrosome and microtubule dynamics during early stages of meiosis in mouse oocytes. Mol Hum Reprod 2003;9: 749–756.
19 Laemmli UK. Cleavage of structural proteins during the assembly of the head of bacteriophage T4. Nature 1970;227:680–685.
20 Towbin H, Staehelin T, Gordon J. Electrophoretic transfer of proteins from polyacrylamide gels to nitrocellulose sheets: Procedure and some applications. Proc Natl Acad Sci U S A 1979;76:4350–4354.
21 Czepulkowski B. Basic techniques for the preparation and analysis of chromosomes from bone marrow and leukemic blood. In: Rooney D, ed. Human Cytogenetics. Malignancy and Acquired Abnormalities. 3rd ed. Oxford, U.K.: Oxford University Press, 2001;15–16.
22 Johnstone B, Hering TM, Caplan AI et al. In vitro chondrogenesis of bone marrow-derived mesenchymal progenitor cells. Exp Cell Res 1998; 238:265–272.
23 Jones M. Connective tissues and stains. In: Bancroft C, Gamble M, eds. Theory and Practice of Histological Techniques. 5th ed. Edinburg, U.K.: Churchill Livingstone, 2002;139–162.
24 Dennis JE, Merriam A, Awadallah A et al. A quadripotential mesenchymal progenitor cell isolated from the marrow of an adult mouse. J Bone Miner Res 1999;14:700–709.
25 Jones M. Lipids. In: Bancroft C, Gamble M, eds. Theory and Practice of Histological Techniques. 5th ed. Edinburg, U.K.: Churchill Livingstone, 2002;201–230.
26 He G, Pedersen SB, Bruun JM et al. Differences in plasminogen activator inhibitor 1 in subcutaneous versus omental adipose tissue in non-obese and obese subjects. Horm Metab Res 2003;35:178–182.
27 Jaiswal N, Haynesworth SE, Caplan AI et al. Osteogenic differentiation of purified, culture-expanded human mesenchymal stem cells in vitro. J Cell Biochem 1997;64:295–312.
28 Churukian C. Pigments and minerals. In: Bancroft C, Gamble M, eds. Theory and Practice of Histological Techniques. 5th ed. Edinburg, U.K.: Churchill Livingstone, 2002;258–259.
29 Callis G. Bone. In: Bancroft C, Gamble M, eds. Theory and Practice of Histological Techniques. 5th ed. Edinburg, U.K.: Churchill Livingstone, 2002;293.
30 Woodbury D, Schwarz EJ, Prockop DJ et al. Adult rat and human bone marrow stromal cells differentiate into neurons. J Neurosci Res 2000; 61:364–370.
31 Temin HM. Studies on carcinogenesis by avian sarcoma viruses. 3. The differential effect of serum and polyanions on multiplication of uninfected and converted cells. J Natl Cancer Inst 1966;37:167–175.
32 Kierszenbaum A. Connective tissue. In: Kierszenbaum A, ed. Histology and Cell Biology. St. Louis: Mosby Inc., 2002;111–112.

33 Castro-Malaspina H, Gay RE, Resnick G et al. Characterization of human bone marrow fibroblast colony-forming cells (CFU-F) and their progeny. Blood 1980;56:289–301.
34 Lazarus HM, Haynesworth SE, Gerson SL et al. Ex vivo expansion and subsequent infusion of human bone marrow-derived stromal progenitor cells (mesenchymal progenitor cells): implications for therapeutic use. Bone Marrow Transplant 1995;16:557–564.
35 Reyes M, Verfaillie CM. Characterization of multipotent adult progenitor cells, a subpopulation of mesenchymal stem cells. Ann N Y Acad Sci 2001;938:231–233; discussion 233–235.
36 Wai LK. Telomeres, telomerase, and tumorigenesis—a review. Med Gen Med 2004;6:19.
37 Herrmann H, Aebi U. Intermediate filaments and their associates: Multitalented structural elements specifying cytoarchitecture and cytodynamics. Curr Opin Cell Biol 2000;12:79–90.
38 Bozhok M, Bannikov GA, Tavokina LV et al. [Local expression of cytokeratins 8, 17 and 18 in the mesenchyme and smooth muscles in the early stages of human organogenesis]. Ontogenez 1989;20:250–257.
39 Moll R, Zimbelmann R, Goldschmidt MD et al. The human gene encoding cytokeratin 20 and its expression during fetal development and in gastrointestinal carcinomas. Differentiation 1993;53:75–93.
40 Kadner A, Zund G, Maurus C et al. Human umbilical cord cells for cardiovascular tissue engineering: A comparative study. Eur J Cardiothorac Surg 2004;25:635–641.
41 Darby I, Skalli O, Gabbiani G. Alpha-smooth muscle actin is transiently expressed by myofibroblasts during experimental wound healing. Lab Invest 1990;63:21–29.
42 Mitchell KE, Weiss ML, Mitchell BM et al. Matrix cells from Wharton's jelly form neurons and glia. STEM CELLS 2003;21:50–60.
43 Wachsmuth L, Soder S, Fan Z et al. Immunolocalization of matrix proteins in different human cartilage subtypes. Histol Histopathol 2006; 21:477–485.
44 Toh WS, Liu H, Heng BC et al. Combined effects of TGFbeta1 and BMP2 in serum-free chondrogenic differentiation of mesenchymal stem cells induced hyaline-like cartilage formation. Growth Factors 2005;23: 313–321.
45 Juhan-Vague I, Alessi MC, Mavri A et al. Plasminogen activator inhibitor-1, inflammation, obesity, insulin resistance and vascular risk. J Thromb Haemost 2003;1:1575–1579.
46 Berberoglu M, Evliyaoglu O, Adiyaman P et al. Plasminogen activator inhibitor-1 (PAI-1) gene polymorphism (-675 4G/5G) associated with obesity and vascular risk in children. J Pediatr Endocrinol Metab 2006; 19:741–748.
47 Sekiya I, Larson BL, Vuoristo JT et al. Adipogenic differentiation of human adult stem cells from bone marrow stroma (MSCs). J Bone Miner Res 2004;19:256–264.
48 Bieback K, Kern S, Kluter H et al. Critical parameters for the isolation of mesenchymal stem cells from umbilical cord blood. STEM CELLS 2004;22:625–634.
49 Chang YJ, Shih DT, Tseng CP et al. Disparate mesenchyme-lineage tendencies in mesenchymal stem cells from human bone marrow and umbilical cord blood. STEM CELLS 2006;24:679–685.
50 Pereira RF, Halford KW, O'Hara MD et al. Cultured adherent cells from marrow can serve as long-lasting precursor cells for bone, cartilage, and lung in irradiated mice. Proc Natl Acad Sci U S A 1995;92:4857–4861.
51 Riederer B, Matus A. Differential expression of distinct microtubule-associated proteins during brain development. Proc Natl Acad Sci U S A 1985;82:6006–6009.
52 Mullen RJ, Buck CR, Smith AM. NeuN, a neuronal specific nuclear protein in vertebrates. Development 1992;116:201–211.
53 Tondreau T, Lagneaux L, Dejeneffe M et al. Bone marrow-derived mesenchymal stem cells already express specific neural proteins before any differentiation. Differentiation 2004;72:319–326.
54 Carden MJ, Trojanowski JQ, Schlaepfer WW et al. Two-stage expression of neurofilament polypeptides during rat neurogenesis with early establishment of adult phosphorylation patterns. J Neurosci 1987;7: 3489–3504.
55 Cattaneo E, McKay R. Proliferation and differentiation of neuronal stem cells regulated by nerve growth factor. Nature 1990;347:762–765.
56 Kirino T, Brightman MW, Oertel WH et al. Neuron-specific enolase as an index of neuronal regeneration and reinnervation. J Neurosci 1983;3: 915–923.
57 Moskowitz PF, Smith R, Pickett J et al. Expression of the class III beta-tubulin gene during axonal regeneration of rat dorsal root ganglion neurons. J Neurosci Res 1993;34:129–134.
58 Banerjee A, Luduena RF. Kinetics of colchicine binding to purified beta-tubulin isotypes from bovine brain. J Biol Chem 1992;267: 13335–13339.
59 Luduena RF. Are tubulin isotypes functionally significant? Mol Biol Cell 1993;4:445–457.
60 Sanchez-Ramos J, Song S, Cardozo-Pelaez F et al. Adult bone marrow stromal cells differentiate into neural cells in vitro. Exp Neurol 2000; 164:247–256.


See www.StemCells.com for supplemental material available online.